Non-uniform splitting of a single mantle plume by double cratonic roots: Insight into the origin of the central and southern East African Rift System

Alexander Koptev, Sierd Cloetingh, Taras Gerya, Eric Calais, Sylvie Leroy

Non-uniform splitting of a single mantle plume by double cratonic roots: Insight into the origin of the central and southern East African Rift System

Alexander Koptev[1,2], Sierd Cloetingh[3], Taras Gerya[4], Eric Calais[5], and Sylvie Leroy[1]

[1]Sorbonne Universités, UPMC Univ Paris 06, CNRS, Institut des Sciences de la Terre de Paris (iSTeP), 4 place Jussieu 75005 Paris, France

[2]Now at Department of Geosciences, University of Tübingen, Tübingen, Germany

[3]Department of Earth Sciences, Utrecht University, Netherlands

[4]ETH-Zurich, Institute of Geophysics, Sonnegstrasse 5, Zurich, Switzerland

[5]Ecole Normale Supérieure, Dept. of Geosciences, PSL Research University, CNRS UMR 8538, Paris, France

Corresponding author: Alexander Koptev, Department of Geosciences, University of Tübingen, Wilhelmstrasse 56, D-72074 Tübingen, Germany.

e-mail: alexander.koptev@ifg.uni-tuebingen.de.

Short title (running head): **Non-uniform splitting of a mantle plume by cratons**

Abstract

Using numerical thermo-mechanical experiments we analyze the role of active mantle plume and pre-existing lithospheric thickness differences in the structural development of the central and southern East African Rift system. The plume-lithosphere interaction model setup captures the essential features of the studied area: two cratonic bodies embedded into surrounding lithosphere of normal thickness. Results of numerical experiments suggest that localization of rift branches in the crust is mainly defined by the initial position of the mantle plume relative to the cratons. We demonstrate that development of the Eastern branch, the Western branch and the Malawi rift can be the result of non-uniform splitting of the Kenyan plume that has been rising underneath the southern part of the Tanzanian craton. Major features associated with Cenozoic rifting can thus be reproduced in a relatively simple context of the interaction between a single mantle plume and pre-stressed continental lithosphere with double cratonic roots.

Introduction

The East African Rift system (EARS) (McConnell, 1972; Chorowicz, 2005; Braile et al., 2006; Ring, 2014) has two branches, the Eastern branch and Western branch. The N-S oriented Eastern branch (Baker et al., 1972; Williams, 1982; Baker, 1987; Keller et al., 1991; Smith, 1994; Mechie et al., 1997; Ebinger, 2005) extends over 2000 km from the Afar Triple Junction (Mohr, 1970; McClusky et al., 2003) in the north to the North Tanzanian Divergence Zone (Dawson, 1992; Le Gall et al., 2004, 2008; Isola et al., 2014) in the south (Figure 1) and consists of the relatively narrow Main Ethiopian rift (Keranen et al., 2009), the wide rift in the Turkana depression (Morley et al., 1992) and a narrow rift at the Tanzanian craton margin in the Kenya rift (Zeyen et al., 1997). In the present study, however, we consider only the southern part of the Eastern branch from Northern Kenya to North-Eastern Tanzania. The Western branch (Ebinger, 1989; Pasteels et al., 1989; Daly et al., 1989; Morley et al., 1999; Bauer et al., 2013) is composed by the Albert-Edward, Kivu and Tanganyika-Rukwa rifts stretched in NE-SW, N-S and NW-SE directions, respectively, depicting an arcuate map-trace along the western side of the Tanzanian craton (Figure 1). The southern prolongation of the Western branch is represented by the Malawi rift (Ring et al., 1992; Laó-Dávila et al., 2015) that is aligned on a N-S trend extending from the Rungwe volcanic province (southern Tanzania) to the Urema graben (Mozambique). Geological estimates indicate a higher degree of total lithospheric extension in the Kenya rift as compared to the Western branch and the North Tanzanian Divergence Zone (Ring, 2014 and references therein).

The Western and Eastern branches are separated by the Archaean (2500-3000 Ma) Tanzanian craton (Bell and Dodson, 1981; Chesley et al., 1999; Manya, 2011) characterized by a strong and cold lithosphere with a 150-300-km-thick keel (Artemieva, 2006; Adams et al., 2012; Mulibo and Nyblade, 2013a,b). The 175-km-thick (Artemieva, 2006) Archaean-Paleoproterozoic Bangweulu block (Andersen and Unrug, 1984; De Waele et al., 2006) that is stable since 1750 Ma (Lenoir et al., 1994), lies to the south-west of the Tanzanian craton. The Tanzanian and Bangweulu cratons are both surrounded by Proterozoic orogenic belts (Cahen et al., 1984; Begg et al., 2009) with a relatively thin (≤150 km) thermal lithosphere (Artemieva, 2006; Koptev and Ershov, 2011).

Geophysical (e.g., Ritsema et al., 1998; Nyblade et al, 2000; Nolet et al., 2006) and geochemical (e.g., Rooney et al., 2012; Armitage et al., 2015) observations indicate the presence of mantle plumes under the EARS, possibly rooted into a common deep mantle anomaly (Ritsema et al., 1999) corresponding to the African superplume. However, the actual number of plumes and their relative position within this broad upwelling region remain contentious (e.g., Weeraratne et al., 2003; Chang and Van der Lee, 2011; Chang et al., 2015; Civiero et al., 2016).

It is commonly assumed that the Cenozoic rifts have avoided the cratons and follow the mobile belts (McConnell, 1972; Mohr, 1982) which serve as the weakest pathways for rift propagation. Structural control of the pre-existing heterogeneities within the Proterozoic belts at the scale of individual faults or rifts has been demonstrated as well (Versfelt and Rosendahl, 1989; Ring, 1994; Theunissen et al., 1996; Corti et al., 2007; Morley, 2010; Katumwehe et al., 2015; Smets et al., 2016).

However, as shown by Koptev et al. (2015, 2016), the formation of two rift zones on opposite sides of a thick lithosphere segment can be explained without appealing to pre-imposed heterogeneities at the crustal level. These models have provided a unified physical framework to understand simultaneous development of the Western and Eastern branches around a thicker Tanzanian craton (Roberts et al., 2012) as a result of the interaction between pre-stressed continental lithosphere and single mantle plume anomaly corresponding to the Kenyan plume (George et al., 1998; Pik et al., 2006; Chang and Van der Lee, 2011). Yet, the southern prolongation of the Western rift by the Malawi rift has not been reproduced in any of these "one-craton" experiments (Koptev et al., 2015, 2016). In order to overcome this discrepancy, we follow-up on our previous studies with a series of laterally widened thermo-mechanical models characterized by a presence of a second zone of lithospheric thickening that roughly mimics the isometric (i.e. having equal horizontal dimensions) Bangweulu block situated south-west of the Tanzanian craton and by a single mantle plume seeded underneath the southern part of the Tanzanian craton (e.g., Hansen et al., 2012; Bagley and Nyblade, 2013).

Model and experiments

Our modeling is based on the thermo-mechanical viscous-plastic 3DELVIS code (Gerya and Yuen, 2007) that combines the finite difference method with a marker-in-cell technique (see Gerya (2010) for more details).

The 3D model box encompasses the entire 650-km-deep upper mantle, with large horizontal scales (2000 × 2000 km) and offers “lithospheric-scale” resolution (~ 5 km × 5 km × 5 km per grid cell). The initial model setup corresponds to onset of a stratified three-layer (upper/lower crust and lithospheric mantle) continental lithosphere which is underlain by asthenospheric upper mantle. The initial geotherm is piece-wise linear, with 0°C at the surface, 700°C at the Moho, 1300°C at the lithosphere-asthenosphere boundary and 1630°C at the bottom of the model box. The mantle plume is initiated by a temperature anomaly of +370°C at the base of the upper mantle. In all presented experiments we have applied a constant extension in E-W direction with a half rate of 3 mm/year, a typical value for pre-break-up continental rifts including the Nubia-Somalia plate system (Stamps et al., 2008; Saria et al., 2014).

The general model series (Table 1; models **1-13**) is characterized by lateral homogeneity of the crustal composition and by presence of two zones of 250 km-thick cratons embedded into surrounding “normal” (150 km-thick) lithosphere. The first cratonic block is elongated in a N-S direction (horizontal dimensions are 400 × 800 km) roughly mimicking the configuration of the Tanzanian craton whereas the second one is small and isometric (horizontal dimensions are 400 × 400 km) corresponding to the Bangweulu block. The initial plume location represents a key controlling parameter of our study (Figure 2). In all performed experiments (except for “no-plume” model **1**; Figure 3) the mantle plume has been shifted to the south up to 230 km with respect to the center of the Tanzanian craton. We have studied the impact of small lateral variations in its initial position: a southward shift varies from 210 km to 230 km whereas latitudinal displacement is from 10 km to the west to 30 km to the east; different configurations of the Tanzanian craton have been tested as well (Table 1; Figures 4-5). In order to investigate the potential role of second-order structural heterogeneities we have performed several complementary experiments (models **14-17**, Figure 6) including stronger (plagioclase flow law instead of wet quartzite flow law) lower crust within the cratonic blocks (models **16-17**) and/or third zone of lithospheric thickening situated to the west of the Tanzanian craton and roughly mimicking the size and configuration of the Masai block (models **14-15**, **17**).

Results and discussions

Similarly to previous 3D experiments (Burov and Gerya, 2014; Koptev et al., 2015, 2016), the models presented here predict a rapid mantle ascent as the mantle plume reaches the lithospheric bottom after 0.5 Myr. The common point of the performed models is a separation of the upwelling plume head into three parts by the lithosphere of the Tanzanian and Bangweulu blocks. After being divided, the buoyant plume material ponds at the base of "normal" lithosphere adjacent to the western, eastern and southern sides of the Tanzanian craton (Figure 4).

In absence of active mantle upwelling ("no-plume" model **1**), ultra-slow tectonic extension can only result in broadly distributed small-offset parallel faults (Figure 3). On the contrary, in most of the other experiments (Figure 4), the continental crust above the hot plume material is subjected to localized brittle deformation forming three linear, 100-500 km-long rifting centers stretched in the direction perpendicular to external E-W extension. As already shown by Burov and Gerya (2014), such large-scale linear normal faults are triggered and maintained by mantle flow that impacts the bottom of continental lithosphere.

The degree of development (in terms of modeled strain rates) of each of these branches is directly controlled by the relative amount of hot plume material ponding underneath the corresponding lithosphere segment (Figure 4). In certain cases, however, this amount appears to be too small to localize any visible deformation in the crust. For example, the plume's eastward shift of 10 km in combination with the simplified shape of the Tanzanian craton results in the absence of a discernible western rift (model **4**, Figure 4c). Similarly, the eastern branch is not reproduced in the experiments assuming a more realistic Tanzanian craton and the mantle plume with initial latitudinal displacement of 0 km or 10 km to the west (models **6** and **5**, respectively; Figure 4e and Figure 4d). Only the plume's eastward shift up to 20 km (models **8-10**; Figure 4g-i) can provide a symmetrical rifting on both (eastern and western) sides of the Tanzanian craton. Further plume displacement to the east (up to 30 km) leads to a more developed eastern branch comparing to the western one (models **11-13**; Figure 4j-l). The southern rift zone situated east of the Bangweulu block is expressed clearly in all models. Note, however, that it becomes less pronounced when the plume's southward shift decreases from 230 km to 210 km (compare models **8** (Figure 4g) and **10** (Figure 4i) or models **11** (Figure 4j) and **13** (Figure 4l)). The asymmetrical distribution of hot mantle material on the opposite sides of the craton (e.g., models **11-12**) can provoke contrasted magmatic activity as observed in the central EARS, explaining a magma-rich Eastern branch and magma-poor Western branch (e.g., Chorowicz et al., 2005; Ring, 2014).

We have identified model **9** (Figure 4h; Figure 5) as the "best-fit" experiment of the general model series (models **1-13**) because it reproduces all three rift zones that are clearly reflected not only in strain rate field but also in the surface topography (Figure 5c). Several other models (such as models **3** or **8**), however, could also be considered as the "best-fit" (Figure 4b,g) because they are able to reproduce a synchronous growth of the Eastern branch, the Western branch and the Malawi rift as well. Note that modeled accumulated deformation in the localized rift basins amounts to several tens km of total extension, that is in accord with geological estimates for the central part of the EARS (e.g.. Ring, 2014 and references therein). A striking feature is the consistency between modeled and observed rift distribution in case of the Kenyan plume seeded underneath the southern part of the Tanzanian craton.

A principal shortcoming of this “best-fit” experiment (model **9**; Figure 5) is that it does not reproduce the NW-SE oriented Rukwa rift segment of the Western branch (Figure 1). Similarly to most of the other models, the southern end of the western branch penetrates into the area underlain by the Bangweulu block. In this case, thick lithosphere appears to be not resistant to lateral propagation of localized deformation given homogenous crustal composition adopted in the general model series when crustal rheology of the cratonic blocks does not differ from surrounding “normal” lithosphere. The situation changes completely when not only thicker lithospheric mantle but also stronger rheology of the lower crust is considered for the cratonic areas (complementary model series: models **16**-**17**, Figure 6c,d): in this case, localized strain tends to avoid the strong cratons keeping them almost undeformed. In particular, this leads to the change of orientation from N-S to NW-SE for the southernmost segment of the western branch (corresponding to the Rukwa rift) thus providing a framework much more consistent with the observed data. Introduction of the Masai block, for its part, improves the relative location of widening of the rift zone in the southern segment of the eastern branch (models **15**, **17**; Figure 6b,d) that would correspond to the observed transition between the narrow Kenya rift to a considerably wider zone (300-400 km) of block faulting in northern Tanzania (Dawson, 1992; Ebinger et al., 1997; Foster et al., 1997; Le Gall, 2008; Corti et al., 2013).

It should be noted that given the better fit with the observed data in case of complementary models containing more predefined complexities (see Figure 6d), the analyzed plume-induced multi-branch continental rifting dynamics need further numerical investigation and quantitative analysis of the controlling factors including complex 3D structure of the central

EARS in terms of inherited compositional and rheological heterogeneities of the crust and lithospheric mantle (e.g., Sippel et al., 2017).

Conclusions

The fully-coupled thermo-mechanical models presented here start from relatively simple initial conditions: a single mantle plume anomaly seeded underneath the continental lithosphere embedding two cratonic blocks. These experiments evolve over time to create a complex system characterized by asymmetrical splitting of the plume head into three parts. The resulting relative distribution of hot plume material ponding below "normal" lithosphere is a controlling parameter for deformation localization at the crustal level. Very small variations in initial plume position with respect to cratonic bodies (up to several tens km only) appear to be able to change the relation between these three segments of separated plume head that, in turn, alters the degree of development of corresponding rift branches. We argue, thus, that the resulting rifting pattern is largely controlled by relative position of the initial mantle plume anomaly with respect to first-order lithospheric thickness differences rather than by second-order crustal and/or lithospheric compositional heterogeneities as commonly assumed before (Theunissen et al., 1996; Corti et al., 2007; Katumwehe et al., 2015; Smets et al., 2016).

The performed analysis permits to identify an initial model configuration that results in a strain distribution that bears strong similarities with the central and southern EARS showing simultaneous development of the Eastern branch, the Western branch and its southern prolongation by the Malawi rift. The number and relative positions of rift branches with respect to the cratons within the studied area can be explained by an impact of single mantle anomaly on pre-stressed continental lithosphere that does not contain any pre-defined heterogeneities other than the well-known cratonic blocks.

Acknowledgments

We thank Judith Sippel and two anonymous reviewers for their helpful comments in the preparation of this paper. A. Koptev acknowledges support from the ERC Advanced Grant 290864 RHEOLITH and ERC Consolidator Grant 615703 EXTREME. S. Cloetingh was supported through a UPMC visiting professor grant. E. Calais acknowledges support from U.S. National Science foundation grant EAR-0538119 and French INSU197 CNRS program Tellus-Rift. The numerical simulations were performed on the ERC-funded SGI Ulysse cluster of ISTEP.

References

Adams, A., Nyblade, A. and Weeraratne, D., 2012. Upper mantle shear wave velocity structure beneath the East African plateau: evidence for a deep, plateauwide low velocity anomaly. *Geophysical Journal International*, **189**, 123-142.

Albaric, J., Déverchère, J., Petit, C., Perrot, J. and Le Gall B., 2009. Crustal rheology and depth distribution of earthquakes: insights from the central and southern East African Rift System. *Tectonophysics*, **468**, 28-41.

Andersen, L.S. and Unrug, R., 1984. Geodynamic evolution of the Bangweulu Block, northern Zambia. *Precambrian Research*, **25**, 187-212.

Armitage, J.J., Ferguson, D.J., Goes, S., Hammond, J.O.S., Calais, E., Rychert, C.A. and Harmon, N., 2015. Upper mantle temperature and the onset of extension and break-up in Afar, Africa. *Earth and Planetary Science Letters*, **418**, 78-90.

Artemieva, I.M., 2006. Global 1×1 thermal model TC1 for the continental lithosphere: implications for lithosphere secular evolution. *Tectonophysics*, **416**, 245-277.

Bagley, B. and Nyblade, A.A., 2013. Seismic anisotropy in eastern Africa, mantle flow, and the African superplume. *Geophysical Research Letters*, **40**, 1500-1505.

Baker, B.H., Mohr, P.A. and Williams, L.A.J., 1972. Geology of the eastern rift system of Africa. *Geological Society of America Special Papers*, **136**, 1-68.

Baker, B.H., 1987. Outline of the petrology of the Kenya rift alkaline province. *Geological Society, London, Special Publications*, **30**, 293-311.

Bauer, F.U., Glasmacher, U.A., Ring, U., Karl, M., Schumann, A. and Nagudi, B., 2013. Tracing the exhumation history of the Rwenzori Mountains, Albertine Rift, Uganda, using low temperature thermochronology. *Tectonophysics*, **599**, 8-28.

Begg, G.C. et al., 2009. The lithospheric architecture of Africa: Seismic tomography, mantle petrology, and tectonic evolution. *Geosphere*, **5**, 23-50.

Bell, K. and Dodson, M.H., 1981. The geochronology of the Tanzanian Shield. *The Journal of Geology*, **89**, 109-128.

Beniest, A., Koptev, A. and Burov, E., 2017a. Numerical models for continental break-up: Implications for the South Atlantic. *Earth and Planetary Science Letters*, **461**, 176-189.

Beniest, A., Koptev, A., Leroy, S., Sassi, W. and Guichet, X., 2017b. Two- branch break- up systems by a single mantle plume: Insights from numerical modeling. *Geophysical Research Letters*, **44**.

Braile, L.W., Keller, G.R., Wendlandt, R.F., Morgan, P. and Khan, M.A., 2006. The East African rift system. *Developments in Geotectonics*, **25**, 213-III.

Burov, E., 2011. Rheology and strength of the lithosphere. *Marine and Petroleum Geology*, **28**, 1402-1443.

Burov, E. and Cloetingh, S., 2010. Plume-like upper mantle instabilities drive subduction initiation. *Geophysical Research Letters*, **37**.

Burov, E. and Gerya, T., 2014. Asymmetric three-dimensional topography over mantle plumes. *Nature*, **513**, 85-89.

Burov, E. and Guillou-Frottier, L., 2005. The plume head–continental lithosphere interaction using a tectonically realistic formulation for the lithosphere. *Geophysical Journal International*, **161**, 469-490.

Burov, E., Guillou-Frottier, L., d'Acremont, E., Le Pourhiet, L. and Cloetingh, S., 2007. Plume head-lithosphere interactions near intra-continental plate boundaries. *Tectonophysics*, **434**, 15-38.

Cahen, L., Snelling, N., Delhal, J. and Vail, J., 1984. *The Geochronology and Evolution of Africa*. Oxford Univ. Press, New York.

Chang, S.J. and Van der Lee, S., 2011. Mantle plumes and associated flow beneath Arabia and East Africa. *Earth and Planetary Science Letters*, **302**, 448-454.

Chang, S.J., Ferreira, A.M.G., Ritsema, J., van Heijst, H.J. and Woodhouse, J.H., 2015. Joint inversion for global isotropic and radially anisotropic mantle structure including crustal thickness perturbations. *Journal of Geophysical Research: Solid Earth*, **120**, 4278-4300.

Chesley, J.T., Rudnick, R.L. and Lee, C.T., 1999. Re-Os systematics of mantle xenoliths from the East African Rift: Age, structure, and history of the Tanzanian craton. *Geochimica et Cosmochimica Acta*, **63**, 1203-1217.

Chorowicz, J., 2005. The east African rift system. *Journal of African Earth Sciences*, **43**, 379-410.

Civiero, C.et al., 2016. Small-scale thermal upwellings under the northern East African Rift from S travel time tomography. *Journal of Geophysical Research: Solid Earth*, **121**, 7395-7408.

Corti, G., Iandelli, I. and Cerca, M., 2013. Experimental modeling of rifting at craton margins. *Geosphere*, **9**, 138-154.

Corti, G., van Wijk, J., Cloetingh, S. and Morley, C.K., 2007. Tectonic inheritance and continental rift architecture: Numerical and analogue models of the East African Rift system. *Tectonics*, **26**.

Daly, M.C., Chorowicz, J. and Fairhead, J.D., 1989. Rift basin evolution in Africa: the influence of reactivated steep basement shear zones. *Geological Society, London, Special Publications*, **44**, 309-334.

Dawson, J., 1992. Neogene tectonics and volcanicity in the North Tanzania Sector of the Gregory Rift Valley: Contrasts with the Kenya sector. *Tectonophysics*, **204**, 81-92.

De Waele, B., Liégeois, J.P., Nemchin, A.A. and Tembo, F., 2006. Isotopic and geochemical evidence of Proterozoic episodic crustal reworking within the Irumide Belt of south-central Africa, the southern metacratonic boundary of an Archaean Bangweulu Craton. *Precambrian Research*, **148**, 225-256.

Ebinger, C., 2005. Continental break-up: the East African perspective. *Astronomy & Geophysics*, **46**, 2-16.

Ebinger, C.J., 1989. Tectonic development of the western branch of the East African rift system. *Geological Society of America Bulletin*, **101**, 885-903.

Ebinger, C., Poudjom, Y., Mbede, E., Foster, F. and Dawson, J., 1997. Rifting Archean lithosphere: The Eyasi-Manyara-Natron rifts, East Africa. *Journal of the Geological Society London*, **154**, 947-960.

Fishwick, S. and Bastow I.D., 2011. Towards a better understanding of African topography: a review of passive-source seismic studies of the African crust and upper mantle. *Geological Society, London, Special Publications*, **357**, 343-371.

Foster, A., Ebinger, C., Mbede, E. and Rex, D., 1997. Tectonic development of the northern Tanzanian sector of the East African Rift System. *Journal of the Geological Society London*, **154**, 689-700.

George, R., Rogers, N. and Kelley, S., 1998. Earliest magmatism in Ethiopia: evidence for two mantle plumes in one flood basalt province. *Geology*, **26**, 923-926.

Gerya, T.V., 2010. *Introduction to Numerical Geodynamic Modelling.* Cambridge University Press, 358 pp.

Gerya, T.V. and Yuen, D.A., 2007. Robust characteristics method for modelling multiphase visco-elasto-plastic thermo-mechanical problems. *Physics of the Earth and Planetary Interiors*, **163**, 83-105.

Hansen, S.E., Nyblade, A.A. and Benoit, M.H., 2012. Mantle structure beneath Africa and Arabia from adaptively parameterized P-wave tomography: Implications for the origin of Cenozoic Afro-Arabian tectonism. *Earth and Planetary Science Letters*, **319**, 23-34.

Huismans, R.S. and Beaumont, C., 2007. Roles of lithospheric strain softening and heterogeneity in determining the geometry of rifts and continental margins. In: *Imaging, Mapping and Modelling Continental Lithosphere Extension and Breakup* (Karner, G.D., Manatschal, G.D., Pinheiro, L.M., eds). *Geological Society, London, Special Publications*, **282**, 111-138.

Isola, I., Mazzarini, F., Bonini, M. and Corti, G., 2014. Spatial variability of volcanic features in early-stage rift settings: the case of the Tanzania Divergence, East African rift system. *Terra Nova*, **26**, 461-468.

Katumwehe, A.B, Abdelsalam, M.G. and Atekwana, E.A., 2015. The role of pre-existing Precambrian structures in rift evolution: The Albertine and Rhino grabens, Uganda. *Tectonophysics*, **646**, 117-129.

Keller, G.R., Khan, M.A., Morganc, P., Wendlandt, R.F., Baldridge, W.S., Olsen, K.H., Prodehl, C. and Braile, L.W., 1991. A comparative study of the Rio Grande and Kenya rifts. *Tectonophysics*, **197**, 355-371.

Keranen, K.M., Klemperer, S.L., Julia, J., Lawrence, J.F. and Nyblade, A.A., 2009. Low lower crustal velocity across Ethiopia: Is the Main Ethiopian Rift a narrow rift in a hot craton? *Geochemistry Geophysics Geosystems*, **10**, Q0AB01.

Koptev, A., Burov, E., Calais, E., Leroy, S., Gerya, T., Guillou-Frottier, L. and Cloetingh, S., 2016. Contrasted continental rifting via plume-craton interaction: Applications to Central East African Rift. *Geoscience Frontiers*, **7**, 221-236.

Koptev, A., Burov, E., Gerya, T., Le Pourhiet, L., Leroy, S., Calais, E. and Jolivet, L., 2017a. Plume-induced continental rifting and break-up in ultra-slow extension context: Insights from 3D numerical modeling. *Tectonophysics*, doi.org/10.1016/j.tecto.2017.03.025.

Koptev, A., Calais, E., Burov, E., Leroy, S. and Gerya, T., 2015. Dual continental rift systems generated by plume-lithosphere interaction. *Nature Geoscience*, **8**, 388-392.

Koptev, A., Cloetingh, S., Burov, E., François, T. and Gerya, T., 2017b. Long-distance impact of Iceland plume on Norway's rifted margin. *Scientific Reports*, **7**.

Koptev A.I. and Ershov A.V., 2011. Thermal thickness of the Earth's lithosphere: a numerical model. *Moscow University Geology Bulletin*, **66**, 323-330.

Laó-Dávila, D.A., Al-Salmi, H.S., Abdelsalam, M.G. and Atekwana, E.A., 2015. Hierarchical segmentation of the Malawi Rift: The influence of inherited lithospheric heterogeneity and kinematics in the evolution of continental rifts. *Tectonics*, **34**, 2399-2417.

Le Gall, B., Gernigon, L., Rolet, J., Ebinger, C., Gloaguen, R., Nilsen, O., Dypvik, H., Deffontaines, B. and Mruma, A., 2004. Neogene-Holocene rift propagation in central

Tanzania: Morphostructural and aeromagnetic evidence from the Kilombero area. *Geological Society of America Bulletin*, **116**, 490-510.

Le Gall, B., Nonnotte, P., Rolet, J., Benoit, M., Guillou, H., Mousseau-Nonnotte, M., Albaric, J. and Deverchère, J., 2008. Rift propagation at craton margin: Distribution of faulting and volcanism in the North Tanzanian Divergence (East Africa) during Neogene times. *Tectonophysics*, **448**, 1-19.

Lenoir, J.L., Liégeois, J.P., Theunissen, K. and Klerkx, J., 1994. The Palaeoproterozoic Ubendian shear belt in Tanzania: geochronology and structure. *Journal of African Earth Sciences*, **19**, 169-184.

Manya, S., 2011. Nd-isotopic mapping of the Archaean–Proterozoic boundary in southwestern Tanzania: Implication for the size of the Archaean Tanzania Craton. *Gondwana Research*, **20**, 325-334.

McClusky, S., Reilinger, R., Mahmoud, S., Sari, D.B. and Tealeb, A., 2003. GPS constraints on Africa (Nubia) and Arabia plate motions. *Geophysical Journal International*, **155**, 126-138.

McConnell, R.B., 1972. Geological development of the rift system of eastern Africa. *Geological Society of America Bulletin*, **83**, 2549-2572.

Mechie, J., Keller, G.R., Prodehl, C., Khan, M.A. and Gaciri, S.J., 1997. A model for the structure, composition and evolution of the Kenya rift. *Tectonophysics*, **278**, 95-119.

Mohr, P., 1982. Musings on continental rifts. In: *Continental and oceanic rifts* (G. Palmason, ed). *American Geophysical Union Geodynamics Series*, **8**, 293-309.

Mohr, P.A., 1970. The Afar Triple Junction and sea-floor spreading. *Journal of Geophysical Research*, **75**, 7340-7352.

Morley, C.K., 2010. Stress re-orientation along zones of weak fabrics in rifts: An explanation for pure extension in ‘oblique’ rift segments? *Earth and Planetary Science Letters*, **297**, 667-673.

Morley, C.K., Cunningam, S.M., Wescott, W.A. and Harper, R.M., 1999. Geology and geophysics of the Rukwa rift. In: *Geoscience of Rift Systems - Evolution of East Africa* (C.K. Morley, ed). *AAPG Studies in Geology*, **44**, 91-110.

Mulibo, G.D. and Nyblade, A.A., 2013a. The P and S wave velocity structure of the mantle beneath eastern Africa and the African superplume anomaly. *Geochemistry, Geophysics, Geosystems*, **14**, 2696-2715.

Mulibo, G.D. and Nyblade, A.A., 2013b. Mantle transition zone thinning beneath eastern Africa: Evidence for a whole-mantle superplume structure. *Geophysical Research Letters*, **40**, 3562-3566.

Nolet, G., Karato, S.I. and Montelli, R., 2006. Plume fluxes from seismic tomography. *Earth and Planetary Science Letters*, **248**, 685-699.

Nyblade, A.A., Owens, T.J., Gurrola, H., Ritsema, J. and Langston, C.A., 2000. Seismic evidence for a deep upper mantle thermal anomaly beneath east Africa. *Geology*, **28**, 599-602.

Pasteels, P., Villeneuve, M., De Paepe, P. and Klerkx, J., 1989. Timing of the volcanism of the southern Kivu province: implications for the evolution of the western branch of the East African Rift system. *Earth and Planetary Science Letters*, **94**, 353-363.

Pérez-Gussinyé, M., Metois, M., Fernández, M., Vergés, J., Fullea, J., and Lowry A.R., 2009. Effective elastic thickness of Africa and its relationship to other proxies for lithospheric structure and surface tectonics. *Earth and Planetary Science Letters*, **287**, 152–167.

Pik, R., Marty, B. and Hilton, D.R., 2006. How many mantle plumes in Africa? The geochemical point of view. *Chemical Geology*, **226**, 100-114.

Ring, U., 1994. The influence of preexisting structure on the evolution of the Cenozoic Malawi Rift (East African Rift system). *Tectonics*, **13**, 313-326.

Ring, U., 2014. The East African Rift System. *Austrian Journal Earth Sciences*, **107**, 132-146.

Ring, U., Betzler, C. and Delvaux, D., 1992. Normal vs. strike-slip faulting during rift development in East Africa: the Malawi rift. *Geology*, **20**, 1015-1018.

Ritsema, J., Nyblade, A.A., Owens, T.J. and Langston, C.A., 1998. Upper mantle seismic velocity structure beneath Tanzania, East Africa: Implications for the stability of cratonic lithosphere. *Journal of Geophysical Research*, **103**, 21201-21213.

Ritsema, J., van Heijst, H.J. and Woodhouse, J.H., 1999. Complex shear wave velocity structure imaged beneath Africa and Iceland. *Science*, **286**, 1925-1928.

Roberts, E.M., Stevens, N.J., O'Connor, P.M., Dirks, P.H.G.M., Gottfried, M.D., Clyde, W.C., Armstrong, R.A., Kemp, A.I.S. and Hemming, S., 2012. Initiation of the western branch of the East African Rift coeval with the eastern branch. *Nature Geoscience*, **5**, 289-294.

Saria, E., Calais, E., Stamps, D.S., Delvaux, D. and Hartnady, C.J.H., 2014. Present-day kinematics of the East African Rift. *Journal of Geophysical Research*, **119**, 3584-3600.

Rooney, T.O., Herzberg, C. and Bastow, I.D., 2012. Elevated mantle temperature beneath East Africa. *Geology*, **40**, 27-30.

Sippel, J. et al., 2017. The Kenya rift revisited: insights into lithospheric strength through data-driven 3-D gravity and thermal modelling. *Solid Earth*, **8**, 45.

Smets, B., Delvaux, D., Ross, K. A., Poppe, S., Kervyn, M., d'Oreye, N. and Kervyn, F., 2016. The role of inherited crustal structures and magmatism in the development of rift segments: Insights from the Kivu basin, western branch of the East African Rift. *Tectonophysics*, **683**, 62-76.

Smith, M., 1994. Stratigraphic and structural constraints on mechanisms of active rifting in the Gregory Rift, Kenya. *Tectonophysics*, **236**, 3-22.

Stamps, D.S., Calais, E., Saria, E., Hartnady, C., Nocquet, J.M., Ebinger, C.J. and Fernandes, R.M., 2008. A kinematic model for the East African Rift. *Geophysical Research Letters*, **35**.

Theunissen, K., Klerkx, J., Melnikov, A. and Mruma, A., 1996. Mechanisms of inheritance of rift faulting in the western branch of the East African Rift, Tanzania. *Tectonics*, **15**, 776-790.

Versfelt, J. and Rosendahl, B.R., 1989. Relationships between pre-rift structure and rift architecture in Lakes Tanganyika and Malawi, East Africa. *Nature*, **337**, 354-357.

Weeraratne, D.S., Forsyth, D.W., Fischer, K.M. and Nyblade, A.A., 2003. Evidence for an upper mantle plume beneath the Tanzanian craton from Rayleigh wave tomography. *Journal of Geophysical Research: Solid Earth*, **108**.

Wenker, S. and Beaumont, C., 2016. Effects of lateral strength contrasts and inherited heterogeneities on necking and rifting of continents. *Tectonophysics*, http://dx.doi.org/10.1016/j.tecto.2016.10.011.

Williams, L.A.J., 1982. Physical aspects of magmatism in continental rifts. *Continental and oceanic rifts*, 193-222.

Zeyen, H., Volker, F., Wehrle, V., Fuchs, K., Sobolev, S.V. and Altherr, R., 1997. Styles of continental rifting: crust-mantle detachment and mantle plumes. *Tectonophysics*, **278**, 329-352.

Figure captions

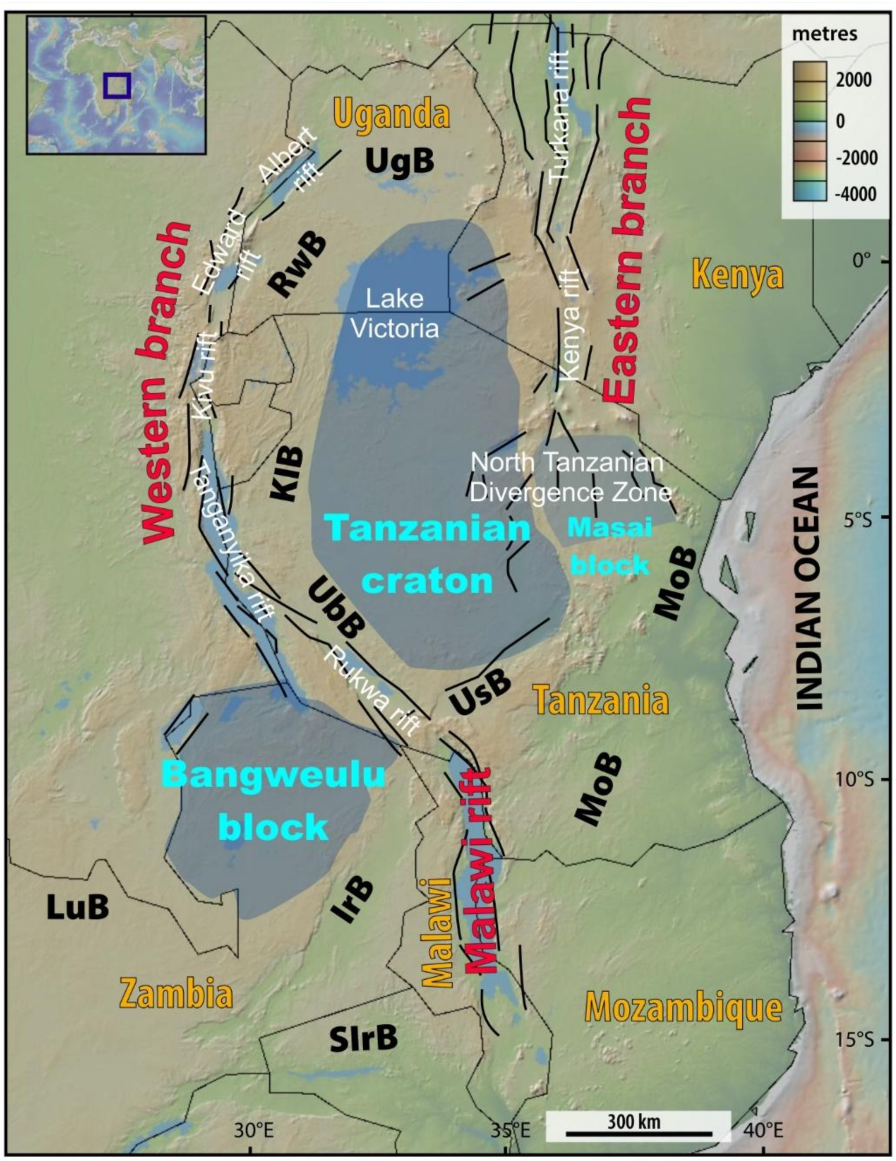

Figure 1. Topographic map showing the tectonic setting of the central and southern EARS (after Mulibo and Nyblade (2013b) and Corti et al. (2013)) that comprises the Tanzanian craton that likely includes the Uganda Basement Complex (UgB), the Bangweulu block, the Masai block and several Proterozoic orogenic belts: Rwenzori (RwB), Kibaran (KiB), Ubendian (UbB), Usagaran (UsB), Mozambique (MoB), Iruminde (IrB), Southern Iruminde (SIrB), Lufilian (LuB). Black lines show major faults (Corti et al., 2013). The inset indicates the location of the studied area.

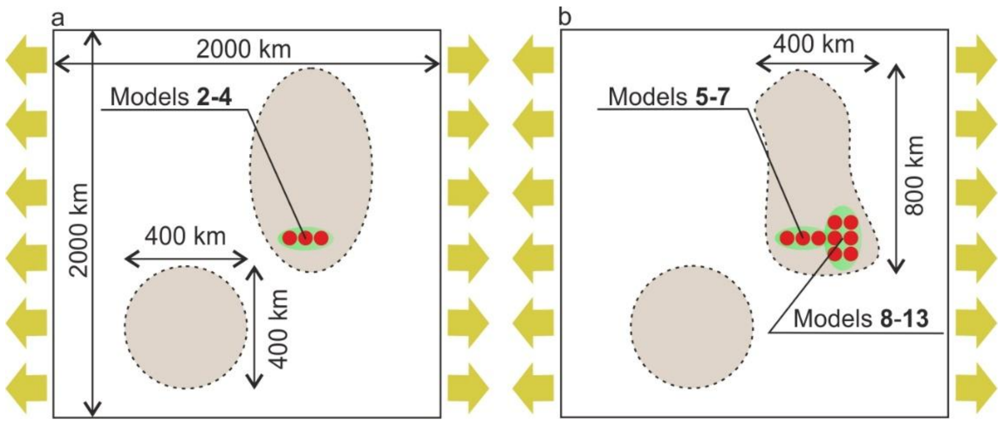

Figure 2. Model setups for the general model series shown on Figure 4: a) the models **2-4**, characterized by a simple quasi-rectangular shape of the Tanzanian craton as in previously published experiments (Koptev et al., 2015, 2016); b) the models **5-13**, with a more complex asymmetrical configuration of the Tanzanian block (based on its present-day surface outline). Initial plume positions are shown by red circles within tested areas (shaded green) with respect to cratonic blocks (gray ellipses). "No-plume" model **1** (see Figure 3) is characterized by simple symmetrical configuration of the Tanzanian craton and by absence of pre-imposed mantle plume anomaly. The initial model setup and geotherm have been adopted with respect to observation-based models of regional thermal and rheological structure of the continental lithosphere in East Africa (Artemieva et al., 2006; Albaric et al., 2009; Pérez-Gussinyé et al., 2009; Fishwick and Bastow, 2011). Rheological parameters have been chosen in consideration of extensive and successful experience obtained from heterogeneous continental rifting (e.g., Huismans and Beaumont, 2007; Wenker and Beaumont, 2016 and references therein) and plume-lithosphere interaction modelling (e.g., Burov and Guillou-Frottier, 2005; Burov et al., 2007; Burov and Cloetingh, 2010; Burov, 2011; Burov and Gerya, 2014; Koptev et al., 2017a,b; Beniest et al., 2017a,b) including our previous Africa-oriented experiments (Koptev et al., 2015, 2016) that have permitted to reproduce a number of key features of the central EARS as timing, surface velocity distribution, and large-scale topography.

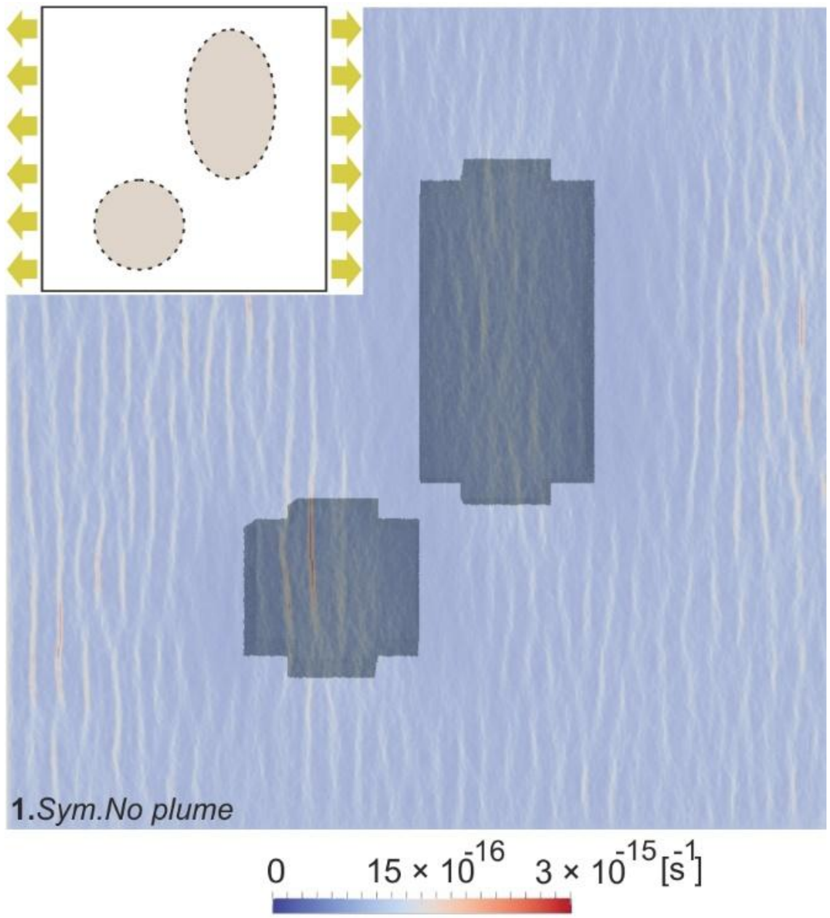

Figure 3. "No-plume" model **1** at 5 Myr. Blue to red colors indicate crustal strain rate. The cratons are the dark gray volumes. Unidirectional tectonic stretching of the continental lithosphere in the absence of active mantle upwelling results in distributed closely spaced small-offset parallel faults, which are not localized within any particular zone. Upper crustal distributed deformation covers all model domains uniformly (including the cratonic areas) because of lateral homogeneity of the crustal composition adopted in the general model series. Note that progressive focusing and amplification of localized non-axisymmetric deformation is generated only by simultaneous presence of the hot plume material underneath the lithosphere basement and passive horizontal extension while mantle plume impingement on non-pre-stressed lithosphere can only result in axisymmetric domal-shaped features with multiple radiating rifts (see Burov and Gerya, 2014 for more detail).

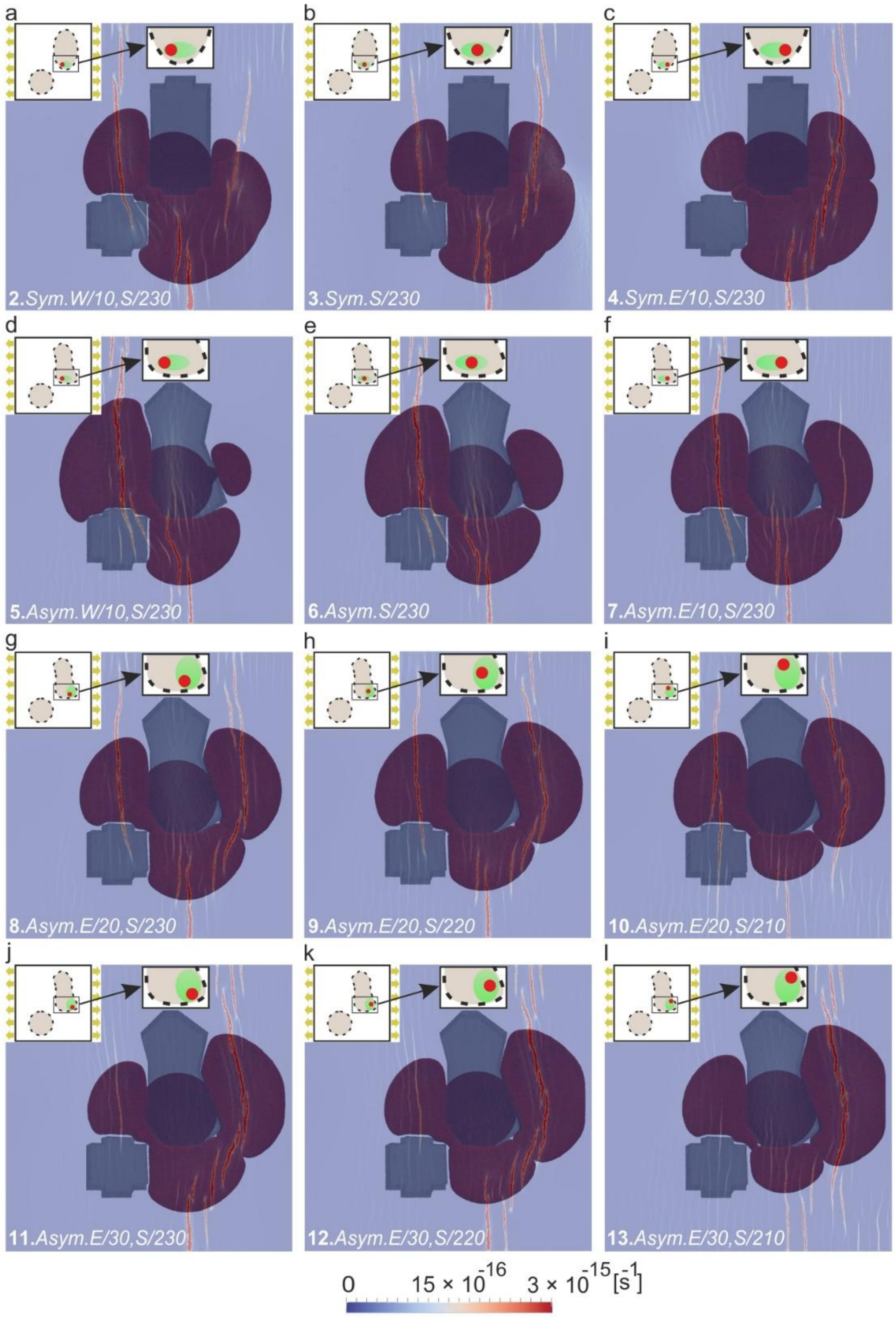

Figure 4. Top view of the results of 3D experiments **2-13** at 5-10 Myr. The plume material is shown in dark red. Left top insets schematically illustrate initial position of the mantle plume. Note that relative position of lithospheric heterogeneities and initial mantle plume anomaly appears to be the crucial factor for resulting rifting pattern.

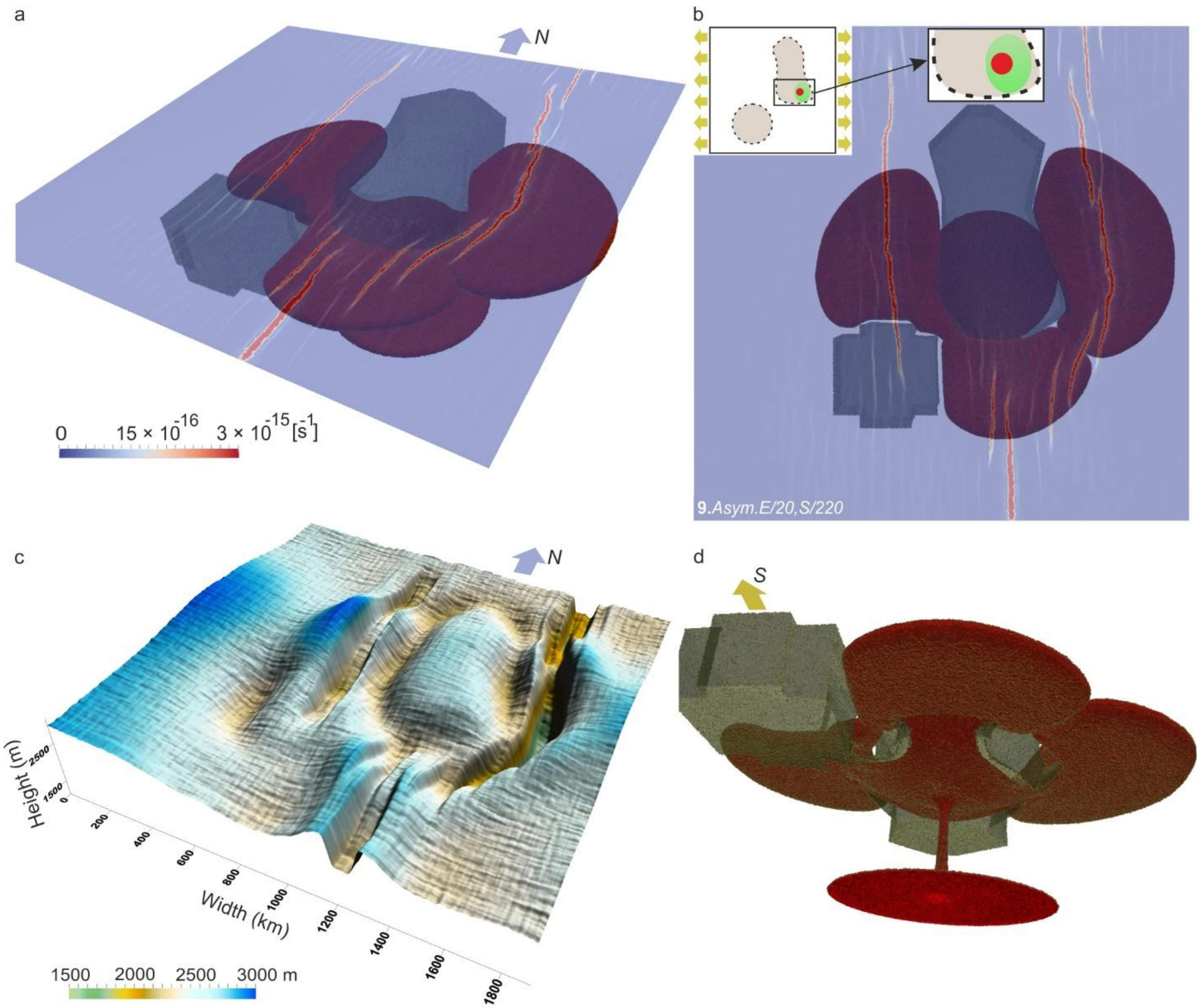

Figure 5. The “best-fit” experiment **9** (*Asym.E/20,S/220*) of the general model series: a) 3D view; b) top view; c) corresponding surface topography; d) bottom view. Note that strain distribution bears strong similarities with the central and southern EARS showing the “three-branches” pattern with simultaneous development of the Eastern branch, the Western branch and the Malawi rift.

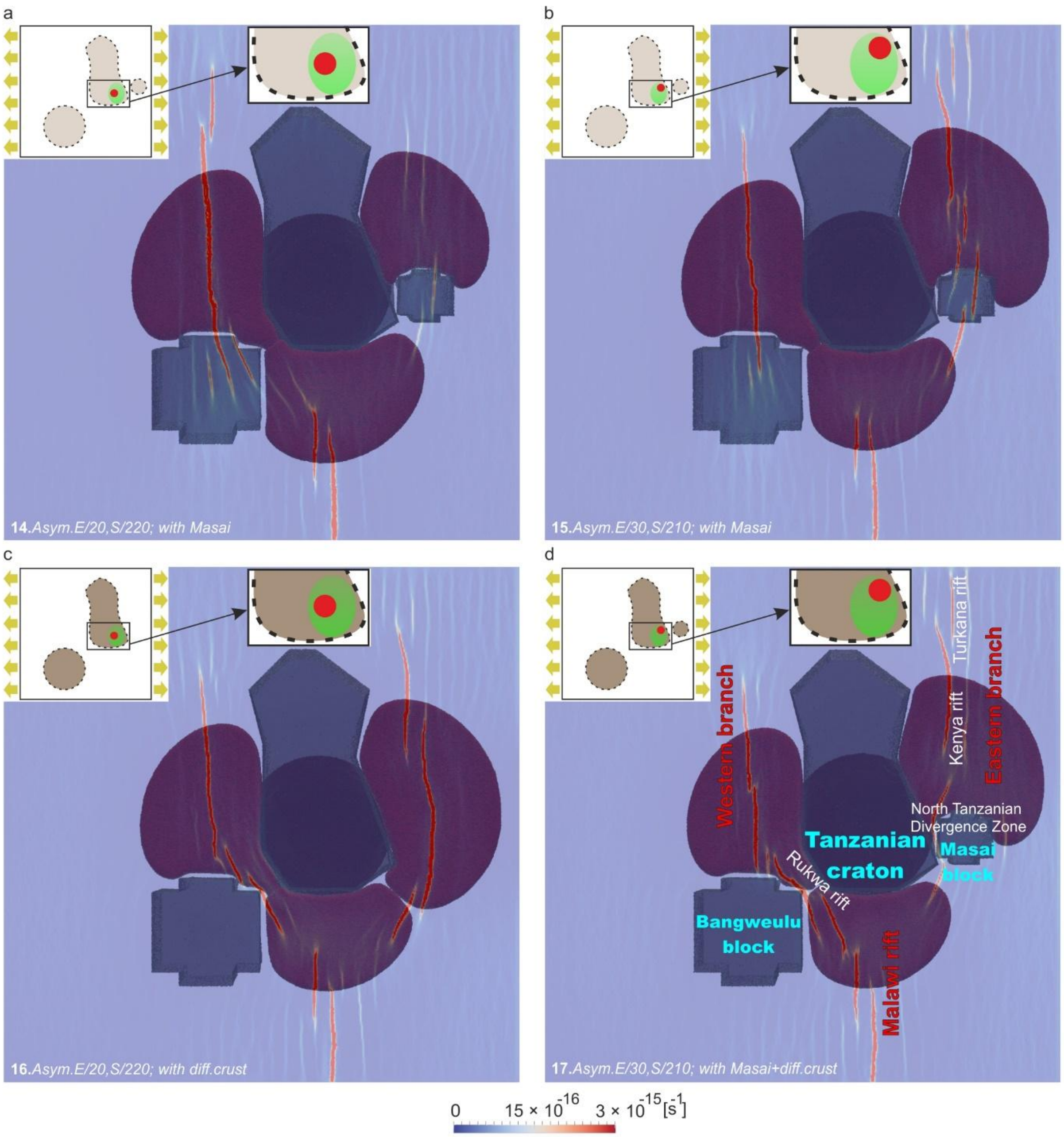

Figure 6. Top view of the complementary models **14-17** at 5-10 Myr. Complementary models differ from the general model series (models **1-13**; Figure 4-5) by: a-b, d) the presence of third area of lithospheric thickening corresponding to the Masai block (models **14-15**, **17**) and/or by c-d) a stronger rheology for the lower crust within cratonic areas (models **16-17**). Note that these experiments containing more predefined complexities provide better fitting with the observed data than in case of the general model series. In particular, the model **17** reproduces not only

three first-order rift structures corresponding to the Eastern branch, the Western branch and the Malawi rift but also such second-order features as NW-SE oriented Rukwa rift and along-axis transition observed between the narrow Kenya rift and the broader Turkana depression to the north and the multi-basin North Tanzania Divergence Zone to the south (compare Figure 1 and Figure 6d).

Table 1. Controlling parameters of the models.

Model number	*Model series*	*Model title*	*Controlling parameters*				*Figure*
			Tanzanian craton shape	*Plume position (az/shift, km)*	*Presence of the Masai block*	*Stronger lower crust for cratons*	
1	General	*Sym.No plume*	Symmetrical	-	No	No	Fig.3
2	General	*Sym.W/10,S/230*	Symmetrical	W/10, S/230	No	No	Fig4a
3	General	*Sym.S/230*	Symmetrical	E/0, S/230	No	No	Fig4b
4	General	*Sym.E/10,S/230*	Symmetrical	E/10, S/230	No	No	Fig4c
5	General	*Asym.W/10,S/230*	Asymmetrical	W/10, S/230	No	No	Fig4d
6	General	*Asym.S/230*	Asymmetrical	E/0, S/230	No	No	Fig4e
7	General	*Asym.E/10,S/230*	Asymmetrical	E/10, S/230	No	No	Fig4f
8	General	*Asym.E/20,S/230*	Asymmetrical	E/20, S/230	No	No	Fig4g
9	General	*Asym.E/20,S/220*	Asymmetrical	E/20, S/220	No	No	Fig4h; Fig.5
10	General	*Asym.E/20,S/210*	Asymmetrical	E/20, S/210	No	No	Fig4i
11	General	*Asym.E/30,S/230*	Asymmetrical	E/30, S/230	No	No	Fig4j
12	General	*Asym.E/30,S/220*	Asymmetrical	E/30, S/220	No	No	Fig4k
13	General	*Asym.E/30,S/210*	Asymmetrical	E/30, S/210	No	No	Fig4l
14	Complementary	*Asym.E/20,S/220; with Masai*	Asymmetrical	E/20, S/220	Yes	No	Fig6a
15	Complementary	*Asym.E/30,S/210; with Masai*	Asymmetrical	E/30, S/210	Yes	No	Fig6b
16	Complementary	*Asym.E/20,S/220; with diff.crust*	Asymmetrical	E/20, S/220	No	Yes	Fig6c
17	Complementary	*Asym.E/30,S/210; with Masai+diff.crust*	Asymmetrical	E/30, S/210	Yes	Yes	Fig6d